


## ARTICLE OPEN



# AraC interacts with p75<sup>NTR</sup> transmembrane domain to induce cell death of mature neurons

Vanessa Lopes-Rodrigues<sup>1,7</sup>, Pia Boxy<sup>2,3,4,7</sup>, Eunice Sim<sup>1</sup>, Dong Ik Park<sup>2,3,4</sup>, Michael Habeck<sup>3,4,5</sup>, Josep Carbonell<sup>6</sup>, Annika Andersson<sup>6</sup>, Diana Fernández-Suárez<sup>6</sup>, Poul Nissen<sup>3,4,5</sup>, Anders Nykjær<sup>2,3,4</sup> and Lilian Kiswa<sup>6</sup> 

© The Author(s) 2023

Cytosine arabinoside (AraC) is one of the main therapeutic treatments for several types of cancer, including acute myeloid leukaemia. However, after a high-dose AraC chemotherapy regime, patients develop severe neurotoxicity and cell death in the central nervous system leading to cerebellar ataxia, dysarthria, nystagmus, somnolence and drowsiness. AraC induces apoptosis in dividing cells. However, the mechanism by which it leads to neurite degeneration and cell death in mature neurons remains unclear. We hypothesise that the upregulation of the death receptor p75<sup>NTR</sup> is responsible for AraC-mediated neurodegeneration and cell death in leukaemia patients undergoing AraC treatment. To determine the role of AraC-p75<sup>NTR</sup> signalling in the cell death of mature neurons, we used mature cerebellar granule neurons' primary cultures from p75<sup>NTR</sup> knockout and p75<sup>NTR</sup>Cys259 mice. Evaluation of neurite degeneration, cell death and p75<sup>NTR</sup> signalling was done by immunohistochemistry and immunoblotting. To assess the interaction between AraC and p75<sup>NTR</sup>, we performed cellular thermal shift and AraTM assays as well as Homo-FRET anisotropy imaging. We show that AraC induces neurite degeneration and programmed cell death of mature cerebellar granule neurons in a p75<sup>NTR</sup>-dependent manner. Mechanistically, Proline 252 and Cysteine 256 residues facilitate AraC interaction with the transmembrane domain of p75<sup>NTR</sup> resulting in uncoupling of p75<sup>NTR</sup> from the NFκB survival pathway. This, in turn, exacerbates the activation of the cell death/JNK pathway by recruitment of TRAF6 to p75<sup>NTR</sup>. Our findings identify p75<sup>NTR</sup> as a novel molecular target to develop treatments for counteract AraC-mediated cell death of mature neurons.

*Cell Death and Disease* (2023)14:440; <https://doi.org/10.1038/s41419-023-05979-7>

## BACKGROUND

AraC (1-β-arabinofuranosylcytosine or cytosine arabinoside) is the most effective chemotherapy agent used to treat patients with acute myeloid leukaemia (AML), as well as other types of haematological cancers [1–5]. In order to achieve the therapeutic efficacy of AraC, patients are subjected to a high-dose AraC (HIDAC) chemotherapy regime [1]. Although HIDAC is efficient in treating AML, it leads to severe cerebellar neurotoxicity [6, 7]. It has been suggested that AraC elicits neurotoxicity by inducing programmed cell death in cerebellar neurons, in particular, cerebellar granule neurons (CGNs) [8, 9]. However, this has only been shown for immature CGNs during development [8, 9]. Noteworthy, AraC-mediated neurotoxicity is prevalent in patients over 50 years old as they are more likely to receive HIDAC [3, 10, 11]. Generally, neuronal proliferation ceases after the developmental period, with the exception of a few brain regions, such as the hippocampus and olfactory bulb [12, 13]. AraC has been shown to induce apoptosis in proliferating cells by inhibiting DNA synthesis [14, 15] and DNA repair [16]. Therefore, it is unlikely that the mechanism by which AraC induces cerebellar

neurotoxicity in adult patients is by targeting proliferating neurons. This warrants the elucidation of the mechanisms by which AraC induces cell death of mature neurons.

The death receptor p75<sup>NTR</sup> is highly expressed in the nervous system during development, but it is widely downregulated in the adult brain [17], with the exception of the cholinergic neurons in the basal forebrain [18]. However, low expression of p75<sup>NTR</sup> persists into adulthood in some areas of the central nervous system (CNS), such as the cerebellum, septum, medulla and pons [19]. Moreover, a growing body of evidence has demonstrated an upregulation of p75<sup>NTR</sup> under pathological conditions, including cancer, brain injury and neurodegenerative diseases [20–23]. Interestingly, an increase in p75<sup>NTR</sup> expression in the serum and peripheral blood of leukaemia patients has been reported [24, 25]. Therefore, we asked whether p75<sup>NTR</sup> could be responsible for mediating AraC-induced neurite degeneration and cell death of mature cerebellar neurons. Here, we show that AraC induces neurite degeneration and apoptosis of mature CGNs by interacting with the transmembrane domain (TMD) of p75<sup>NTR</sup>, an interaction that is dependent on the Proline (Pro) 253 and

<sup>1</sup>Department of Physiology and Life Sciences Institute, National University of Singapore, Singapore 117597, Singapore. <sup>2</sup>Department of Biomedicine, Aarhus University, Aarhus, Denmark. <sup>3</sup>Danish Research Institute of Translational Neuroscience (DANDRITE)–Nordic EMBL Partnership for Molecular Medicine, Aarhus University, Aarhus, Denmark. <sup>4</sup>The Danish National Research Foundation Center, PROMEMO, Aarhus University, Aarhus, Denmark. <sup>5</sup>Department of Molecular Biology and Genetics, Aarhus University, Aarhus, Denmark. <sup>6</sup>Department of Neuroscience, Karolinska Institute, Stockholm S-17177, Sweden. <sup>7</sup>These authors contributed equally: Vanessa Lopes-Rodrigues, Pia Boxy.

<sup>✉</sup>email: [liki@biomed.au.dk](mailto:liki@biomed.au.dk)

Edited by Dr Maria Victoria Niklison Chirou

Received: 22 April 2023 Revised: 29 June 2023 Accepted: 11 July 2023

Published online: 17 July 2023

Cysteine (Cys) 256 residues. Functionally, we show that AraC interaction with the p75<sup>NTR</sup> TMD uncouples p75<sup>NTR</sup> from the NFκB survival pathway, resulting in the exacerbated activation of the cell death/JNK pathway in CGNs.

## MATERIALS AND METHODS

### Animals

Mice were housed in a 12-hour light/dark cycle and fed a standard chow diet. The mutant mouse lines used were p75<sup>NTR</sup> knockout (p75<sup>NTR</sup><sup>-/-</sup>) [26] and p75<sup>NTRCys259</sup> (knock-in mice carrying a substitution of cysteine at position 259 to alanine) [27] mice. Both transgenic mouse lines were maintained on a C57BL/6J background. Mice of both sexes were used for the experiments. All animal experiments were conducted in accordance with the National University of Singapore Institutional Animal Care, Use Committee and the Stockholm North Ethical Committee for Animal Research regulations and the Danish Animal Experiment Inspectorate Under the Ministry of Justice.

### Neuronal cultures

P7 mouse cerebella were dissected with the removal of the meninges in ice-cold phosphate saline buffer (PBS). Whole cerebella were then digested with TrypLE™ Express (Gibco, 12604021) for CGNs extraction. CGNs were plated at a density of 40,000 cells per coverslip coated with poly-D-lysine (Sigma, P1524) in a 24-well plate (Thermo Scientific, 142475) in neurobasal medium (Gibco, 21103049) supplemented with 25 mM KCl, 1 mM Glutamax (Gibco, 35050061), 1× Pen/Strep (Sigma, P4333), 10 μM AraC (Sigma, C-6645), 1× B27 supplement (Gibco, 17504044). AraC was diluted in PBS and used at a concentration of 10 μM for the elimination of glia cells in the neuronal cultures. For experimental conditions, AraC was used at concentrations of 500 and 1000 μM. These high concentrations were used to reflect the high doses (2–3 g/m<sup>2</sup>) of AraC per dose given to patients on a HIDAC chemotherapy regime [28–30]. HIDAC protocol (2–3 g/m<sup>2</sup> every 12 h for up to 6 doses per round of treatment) has been shown to result in AraC concentration exceeding 100 μM in plasma [31].

### Neurite degeneration

To assess neurite degeneration, 4 days in vitro (DIV) wild-type neurons were treated for 24 or 48 h with 500 μM AraC. After treatment, CGNs were fixed for 10 min with ice-cold methanol. Cells were then permeabilized and blocked in 5% normal donkey serum (Jackson ImmunoResearch: 017-000-121) and 0.3% Triton X-100 (Thermo Scientific; 85111) in PBS. Cells were incubated overnight at 4 °C with mouse anti-β-III tubulin (R&D Systems, MAB1195; 1:2500) and counterstained the following day with donkey anti-mouse Alexa Fluor 488 (Abcam, ab150105; 1:2000) and Hoechst (Sigma, B2261; 1:2000). Images were taken using a Confocal Microscope LSM 780 Zeiss Axio Observer fluorescence microscope. Images were captured from regions with well-separated neurites. NIH ImageJ software was used to threshold and binarize the images and remove all cell bodies, after which the Analyse Particles algorithm was applied to identify the area of fragments based on size (20–10,000 pixels) and circularity (0.2–1.0). The degeneration index (DI) was then calculated as the ratio of the total area of detected neurite fragments over the total neurite area. In agreement with previous studies [32], a DI of 0.2 or higher indicated neurite degeneration.

### Cell death

Apoptosis was assessed in WT, p75<sup>NTR</sup><sup>-/-</sup> and p75<sup>NTRCys259</sup> CGNs treated for 24 h with either 500 μM or 1000 μM AraC starting at 4 DIV. Apoptotic cells were labelled using Click-iT plus TUNEL assay for in situ apoptosis detection kit (Thermo Scientific, Cat: C10617) according to manufacturer instructions. Neurons were also stained for cleaved caspase 3 (Cell Signalling Technology, 9761, 1:400), β-III tubulin and DAPI (Sigma; D9542; 1:10,000) following the protocol for immunocytochemistry explained below. For each experiment and treatment, neurons were cultured in duplicates, and at least 15 images were taken per coverslip with a Zeiss Axioplan confocal microscope. The number of cells positive for cleaved caspase 3 and TUNEL was quantified using NIH ImageJ software.

### Protein collection and immunoblotting

To collect protein for immunoblotting, WT neurons were cultured at high density (~200,000 neurons per well) in a 48-well plate. Four days after plating, cells were stimulated with 500 μM AraC for 15, 30 and 60 min.

Protein samples were prepared for SDS-PAGE in SDS sample buffer (Merck Millipore; 70607) and boiled at 95 °C for 10 min before electrophoresis on 12% gels. Proteins were transferred to PVDF membranes (Amersham, GE1060023). Membranes were blocked with 5% non-fat milk and incubated with primary antibodies.

The following primary antibodies were used at the indicated dilutions: rabbit anti-phospho Y515 TrkB (Abcam: ab131483; 1:500), goat anti-TrkB (R&D systems; AF1494; 1:500), rabbit anti-IκBα (Santa Cruz; 9165; 1:500), rabbit anti-phospho-c-Jun (Thr91, Cell Signalling Technology; 2303; 1:1000), rabbit anti-c-Jun (Cell Signalling Technology; 9165; 1:1000) and mouse anti-GAPDH (Sigma; G8795; 1:1000). Immunoreactivity was visualised using appropriate HRP-conjugated secondary antibodies (Cell Signalling Technology; 7074). Immunoblots were developed using the ECL Advance Western blotting detection kit (Thermo Scientific; 34095) and imaged using a chemiluminescent western blot imaging system, Azure c300 (Azure Biosystems). Image analysis and quantification of band intensities were done using NIH ImageJ software.

### RhoA assay

Protein was extracted from WT CGNs that were treated at 4 DIV with 500 μM AraC for 30 min. RhoA activity was evaluated in total CGNs extracts using the RhoA G-Lisa kit (Cytoskeleton; BK124) following the manufacturer's instructions. An equal amount of protein was used from each sample as determined by the BCA protein Assay (ThermoFisher Scientific; 23235).

### Proximity ligation assay (PLA)

Four DIV WT CGNs were treated with 500 μM AraC for 10 min. After treatment, CGNs were fixed for 15 min in 4% paraformaldehyde (PFA)/4% sucrose, permeabilized, and blocked in 10% normal donkey serum and 0.3% Triton X-100 in PBS for 1 h. Neurons were then incubated overnight at 4 °C with anti-p75<sup>NTR</sup> (Promega; G323A; 1:500) and anti-TRAF6 (Santa Cruz; sc-8490; 1:100) antibodies in PBS supplemented with 3% BSA. The Duolink In Situ Proximity Ligation kit (Sigma; DUO92007) was used as per the manufacturer's instructions. Cells were imaged with an LSM Imager Z2 confocal microscope (Zeiss) to detect PLA signals. PLA puncta were quantified using NIH ImageJ software with the plugin particle analyser.

### Immunocytochemistry

For immunocytochemistry, the cultures were fixed in 4% PFA/4% sucrose for 15 min and washed with PBS before blocking nonspecific binding and permeabilizing with blocking solution (5% donkey serum and 0.3% Triton X-100 in PBS) for 1 h at room temperature. Neurons were incubated overnight with the primary antibodies in diluted blocking solution to 1% donkey serum at 4 °C. After washing with PBS, the neurons were incubated with the appropriate secondary antibodies.

The primary antibodies used in this study were: polyclonal anti-cleaved caspase 3 (Cell Signalling Technology; 9761; 1:400), monoclonal anti-β-III tubulin (R&D systems, Cat: MAB1195, 1:10000), polyclonal anti-p75<sup>NTR</sup> (Neuromics; GT15057; 1:500), polyclonal anti-TrkB (R&D systems; AF1494; 1:250), polyclonal anti-MAP2 (Abcam; ab5392; 1:2000) and polyclonal anti-p65NFκB (Santa Cruz; sc-372; 1:250).

Secondary antibodies were Alexa Fluor-conjugated anti-immunoglobulin from Life Technologies and Invitrogen, used at 1:1500 ((donkey anti-rabbit IgG Alexa Fluor 555, (A31572), donkey anti-mouse IgG Alexa Fluor 488 (A21202), donkey anti-mouse IgG Alexa Fluor 555 (A31570), donkey anti-goat IgG Alexa Fluor 488 (A11055), donkey anti-rabbit IgG Alexa Fluor 488 (A32790), donkey anti-chicken IgG Alexa Fluor 647 (703-496-155)). Images were obtained using a Zeiss Axioplan confocal microscope. The number of cells positive for cleaved caspase 3 and TUNEL were quantified using NIH ImageJ software.

### Docking analysis

The nuclear magnetic resonance (NMR) structure of the p75<sup>NTR</sup> TMD dimer in complex with NSC49652 was used for docking of AraC (pdb:5zgg) [33]. NSC49652 was removed, and AutoDock Tools [34] was used for assigning Gasteiger charges and hydrogens to AraC (pdb ligand: AR3). A grid box was centred around the TMD interface, and docking was performed using AutoDock Vina [35], ProteinsPlus [36], PoseView [37] and ChimeraX [38] were used for visualisation of 2D interaction diagrams.

### AraTM assay

AraTM assay was used to assess conformation changes and binding strength in a pair interaction of TMDs [39, 40], as previously described [33].

Briefly, TMD cDNAs of the human p75<sup>NTR</sup> (NLIPVYCSILAAVVVGL-VAYIAFKRW) and TrkB (SVYAVVVIASVVGFCLLVMLFLL) were subcloned into AraTM chimera plasmid in between the KpnI and SacI restriction sites. AS19 LPS-negative *Escherichia coli* cells were transformed with the above-mentioned plasmids together with a GFP reporter plasmid. The selected colonies were grown overnight for 18 h in a shaker at 37°C in Lysogeny Broth (LB) supplemented with 50 µg/ml Spectinomycin and 100 µg/ml ampicillin. The culture was then diluted 1:100 in fresh LB medium and allowed to grow till optical density (OD) 630 reached between 0.2 and 0.5, after which 1 mM IPTG was added to induce the expression of the p75<sup>NTR</sup> TMD–AraTM chimera or TrkB TMD–AraTM chimera. 100 µl of the culture per well was dispensed in black-rim clear bottom 96-well plates (Corning, cat: 3631) previously plated with serial concentrations (30, 100, 300, 500 and 100 µM) of AraC. The plates were then incubated with vigorous shaking at 38°C for 4 h to allow IPTG-induced expression of the TM–AraTM chimera. The plates were then centrifuged at 4000 rpm for 10 min at room temperature to pellet bacteria. LB media was aspirated and replaced with 100 µl of PBS, and bacteria cells were resuspended by vigorous shaking for 10 min. GFP signal was measured in each well (excitation 475 nm, emission 509 nm), and bacterial density was determined by measurement of OD<sub>630</sub> in a microplate plate reader (BioTek).

### Cellular thermal shift assay

Cellular thermal shift assay (CETSA) was performed as previously described [41]. 293 T HEK cells constitutively expressing p75<sup>NTR</sup> protein were homogenised in a buffer containing 100 mM HEPES, 1 mM DTT, 10 mM MgCl<sub>2</sub>, protease inhibitor cocktail tablets (Roche; 11836153001) and phosphatase inhibitors (Roche; 04906837001). After 3 freeze-thaw cycles using liquid nitrogen, the lysate was centrifuged (20,000g, 4 °C, 20 min) to collect the supernatant. Protein concentration was measured using BCA assay. The same amount of protein lysate was aliquoted into different PCR tubes and incubated with either PBS (vehicle) or 500 µM AraC for 3 min at room temperature. The samples were then simultaneously subjected to 6 different temperatures (37, 41, 45, 49, 53 and 57 °C) for 3 min in the Veriti Thermal Cycler (Applied Biosystems). After 3 min cooling on ice, heat-treated protein lysate was centrifuged (20,000g, 4 °C, 20 min). The supernatant was collected into new tubes, and samples were subjected to immunoblotting. Primary antibodies used were anti-p75<sup>NTR</sup> (Promega, Cat: G323A, 1:300). The densitometry was done on the immunoblot bands, and restricted cubic spline curve fitting was generated using GraphPad Prism 9 (GraphPad Software, Inc., La Jolla, CA, USA).

### Isothermal dose response-CETSA (ITDR-CETSA)

The protein lysate from 293 T HEK cells constitutively expressing p75<sup>NTR</sup> protein was homogenised in the same buffer as described above for CETSA and incubated with different concentrations of AraC (0, 0.1, 1, 30, 100, 300, 500 and 1000 µM) for 3 min at RT. The protein extracts were heated at a constant temperature of 37 or 53 °C for 3 min. After subsequent cooling on ice for 3 min, the heat-treated lysate was centrifuged (20,000g, 4 °C, 20 min), followed by supernatant collection. Samples were then subjected to immunoblotting and probed for anti-p75<sup>NTR</sup> (Promega, Cat: G323A, 1:300) and anti-GAPDH (Sigma, Cat: G8795, 1:1000). Densitometry data acquired from 37 °C ITDR-CETSA were used as non-denaturing controls to normalise those from ITDR-CETSA conducted at 53 °C. The densitometry was done on the immunoblot bands, and restricted cubic spline curve fitting was generated using GraphPad Prism 9 (GraphPad Software, Inc., La Jolla, CA, USA).

### Homo-FRET anisotropy imaging

COS-7 cells were cultured under standard conditions in Dulbecco's modified eagle medium (DMEM)-supplemented with 10% foetal bovine serum, 100 units/ml penicillin, 100 mg/ml streptomycin and 2.5 mM glutamate. Cells were transiently transfected with a rat p75<sup>NTR</sup>-EGFP\* fusion constructs [42] using FuGENE transfection reagents (Fisher Scientific, Cat: PRE2311). EGFP\* consist of a monomeric A207K EGFP mutant. 24 h later, anisotropy imaging was done as previously described [27, 33, 43]. Changes in anisotropy were expressed as fold change at each time point in comparison to the mean of 6-time points obtained prior to the addition of the vehicle or 500 µM AraC. Images were acquired using Nikon Ti-E-based live cell epi-fluorescence microscope and MetaMorph software and analysed using MatLab from Mathworks.

### Statistical analysis

Data are expressed as mean and standard errors of the mean. No statistical methods were used to predetermine sample sizes, but our sample sizes are

similar to those generally used in the field. No data were excluded from the analysis. Following the normality test and homogeneity variance (*F*-test or Kolmogorov–Smirnov test with Dallal–Wilkinson–Lilliefors *P* value), group comparison was made using an unpaired student *t*-test, one-way or two-way ANOVA as appropriate followed by Bonferroni post hoc test for normally distributed data. Differences were considered significant for *P* < 0.05. The experiments were not randomised.

## RESULTS

### AraC induces neurite degeneration and apoptosis in mature CGNs

Apoptosis of immature CGNs associated with AraC is well-documented [8, 9, 44–46]. However, it is known that adult cancer patients under AraC medication also develop cerebellar neurotoxicity resulting in neurite degeneration and cell death [6, 7] despite a lack of neurogenesis and proliferation in the adult cerebellum. First, we aimed to confirm that AraC induces degeneration and apoptosis in mature CGNs. To obtain mature neurons for the experiments, we performed P7 cerebellar cultures, initially containing a mixture of glial cells and immature CGNs. To eliminate the proliferating glial cells from the culture, we cultured the cells for 4 days in media containing a low concentration of AraC (10 µM; Fig. 1A), obtaining enriched CGN cultures deprived of glial cells (Supplementary Fig. 1A, B). Previous reports suggested that CGN cultures after 4 DIV contain mature-like neurons that present high expression of mature markers such as MEF2 and Zic2 and low levels of immature markers such as Math1 or TAG1 [47]. We confirmed the maturity of our CGNs by staining for TAG1 (Supplementary Fig. 1C). On the 4 DIV, neurons were treated with either PBS (control) or 500 µM AraC for 24 or 48 h (Fig. 1A). Quantification of the neurite DI showed an increase in neurite degeneration in neurons treated with 500 µM AraC for 24 h compared to untreated neurons (Fig. 1B, C). Longer (48 h) exposure of neurons to 500 µM AraC worsened neurite degeneration (Fig. 1B, D). Moreover, cells treated with either 500 µM or 1000 µM AraC for 24 h showed an increase in the number of cleaved caspase 3 positive neurons (Fig. 1E, F). In agreement with this, analysis of the number of TUNEL analyses showed an approximately 2-fold increase in apoptotic activity in CGNs after either 500 µM or 1000 µM AraC-treatment (Fig. 1G, H), suggesting that the lower concentration is sufficient for reaching the plateau on the apoptotic effect. Therefore, these results are in agreement with previous studies [8, 9, 45], indicating that AraC induces neurite degeneration and cell death of mature CGNs

### p75<sup>NTR</sup> death receptor is required for AraC-induced neurodegeneration and apoptosis in mature CGNs

We and others have shown that the p75<sup>NTR</sup> death receptor plays an important role in CGNs apoptosis during development [48–52]. Although p75<sup>NTR</sup> is abundantly expressed in several types of developing neurons, its expression is negligible in the majority of mature neurons [19, 53].

However, some areas of the adult brain, such as the cerebellum, contain low levels of p75<sup>NTR</sup>. Interestingly, it has also been observed that upon injury and neurodegeneration, p75<sup>NTR</sup> expression is upregulated in the CNS [20, 22, 54]. We, therefore, asked whether the cerebellum is especially vulnerable to AraC-induced cell death due to the presence of p75<sup>NTR</sup> in mature cerebellar neurons. First, we confirmed the expression of p75<sup>NTR</sup> in mature CGNs (Fig. 2A). Next, we assessed whether the addition of AraC to these neurons could trigger the expression of p75<sup>NTR</sup>, therefore increasing their vulnerability to AraC-induced cell death. We found that increasing doses of AraC increased the expression of p75<sup>NTR</sup> in cultured CGNs (Fig. 2B). Then, we tested whether AraC-mediated neuronal death requires p75<sup>NTR</sup>. Wild type (p75<sup>NTR+/+</sup>) and p75<sup>NTR</sup> knockout (p75<sup>NTR-/-</sup>) CGNs were treated at 4 DIV with PBS (control) or AraC for 24 h, and then apoptotic activity was evaluated using cleaved caspase 3 and TUNEL

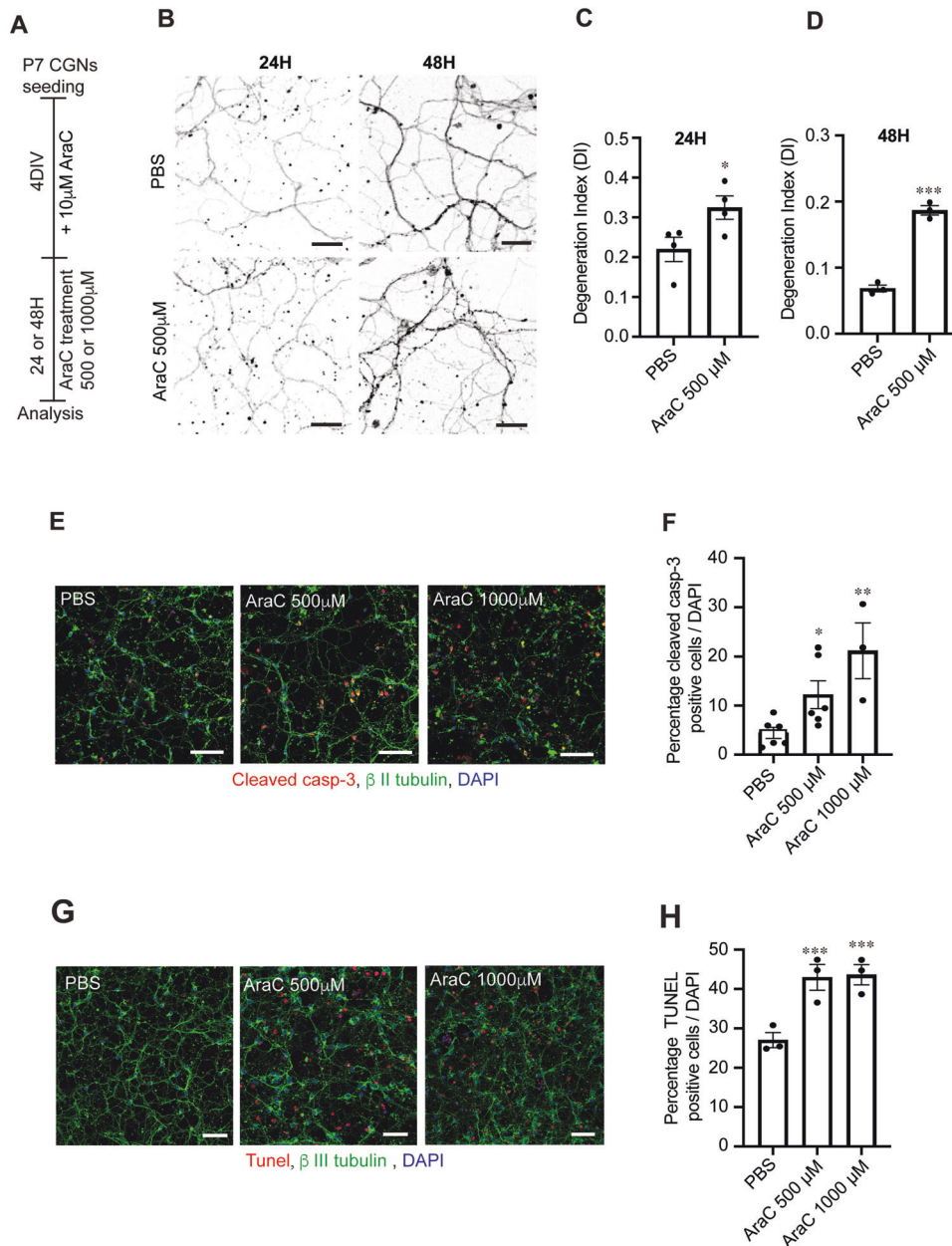


**Fig. 1 AraC induces neurite degeneration and apoptosis in mature CGNs.** **A** A schematic drawing of the cell culture procedure. **B** Image of representative wild-type P7 CGNs neurite grown for 4 DIV that were treated with either PBS (control) or 500  $\mu\text{M}$  AraC for 24 or 48 h and stained for  $\beta$  III tubulin. Scale bars, 50  $\mu\text{m}$ . **C, D** Quantification of degeneration index in CGNs treated with either PBS (control) or 500  $\mu\text{M}$  AraC for 24 h (**C**) and 48 h (**D**) CGNs cultures (total of 25 images per condition were quantified). Mean  $\pm$  s.e.m. of data from 3 to 4 separate cultures ( $*P < 0.05$  and  $***P < 0.001$  compared to control, Unpaired Student *t*-test) is shown. **E** Image of representative P7 CGNs cultured for 4 DIV that were treated with either PBS (control) or 500  $\mu\text{M}$  AraC for 24 h and stained for cleaved caspase 3 (red), anti- $\beta$  III tubulin (green) and counterstained with DAPI (blue). Scale bars, 50  $\mu\text{m}$ . **F** Quantification of percentage cleaved caspase 3 positive neurons in CGNs treated with PBS (control), 500  $\mu\text{M}$  or 1000  $\mu\text{M}$  AraC for 24 h (a total of 80 images per condition were counted). Mean  $\pm$  s.e.m. of data from four separate cultures ( $*P < 0.05$  and  $**P < 0.01$  compared to control, one-way ANOVA followed by Bonferroni post hoc test) is shown. **G** Photomicrographs of representative wild-type P7 CGNs cultured for 4 DIV that were treated with either untreated PBS (control), 500  $\mu\text{M}$  or 1000  $\mu\text{M}$  AraC for 24 h and stained for TUNEL (green), with anti- $\beta$  III tubulin (red) and counterstained with DAPI (blue). Scale bars, 50  $\mu\text{m}$ . **H** Quantification of percentage TUNEL-positive neurons in CGNs treated with PBS, 500  $\mu\text{M}$  or 1000  $\mu\text{M}$  AraC for 24 h (a total of 60 images per condition were counted). Mean  $\pm$  s.e.m. of data from three separate cultures,  $***P < 0.001$  compared to control, one-way ANOVA followed by Bonferroni post hoc test) is shown.

assays. As expected, the number of WT CGNs positive for cleaved caspase 3 (Fig. 2C, D) and TUNEL (Fig. 2C, E) increased 2-fold after AraC treatment.  $p75^{\text{NTR}}/-/-$  neurons treated with AraC did not show an increase in apoptotic activity (Fig. 2C–E). Altogether, these data suggest that AraC-mediated neuronal death requires  $p75^{\text{NTR}}$  death receptor.

#### AraC interacts with $p75^{\text{NTR}}$

Although our data show that in the absence of  $p75^{\text{NTR}}$ , AraC is unable to induce apoptosis in mature neurons, it remains unclear whether this effect was a result of a direct interaction between AraC and  $p75^{\text{NTR}}$  or an indirect effect through  $p75^{\text{NTR}}$  interacting partners. To assess this, we performed an in silico analysis to

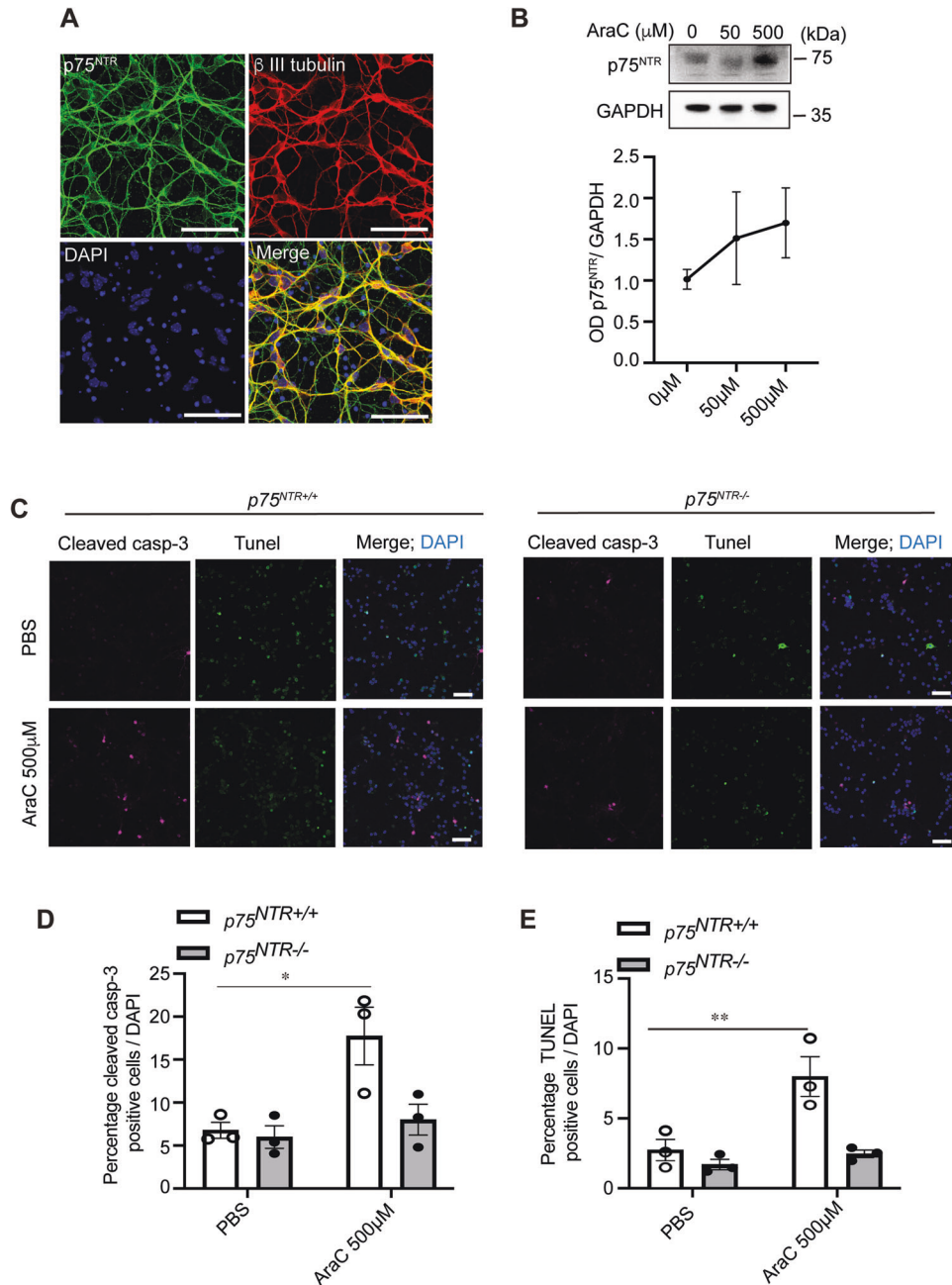


**Fig. 2** AraC requires p75<sup>NTR</sup> to induce apoptosis in mature CGNs. **A** Representative micrographs of wild-type P7 CGNs cultured for 4 DIV and double stained with anti-p75<sup>NTR</sup> together with anti-β III tubulin and counterstained with DAPI. Scale bars, 50 μm. **B** Representative and quantification of immunoblots showing the expression of p75<sup>NTR</sup> in 4DIV CGNs treated with PBS (0 μM AraC), 50 μM or 500 μM AraC for 24 h. **C** Image of representative P7 *p75<sup>NTR</sup>+/+* and *p75<sup>NTR</sup>-/-* CGNs cultured for 4 DIV, treated with either PBS (control) or 500 μM AraC for 24 h and stained for anti-cleaved caspase 3 (magenta), TUNEL (green) and counterstained with DAPI (blue). Scale bars, 50 μm. **D, E** Quantification of percentage cleaved caspase 3 positive (**D**) and TUNEL positive (**E**) in *p75<sup>NTR</sup>+/+* and *p75<sup>NTR</sup>-/-* neurons treated with PBS or AraC (500 μM or 1000 μM for 24 h (total of 80 images per condition were counted)). Mean ± s.e.m. of data from four separate cultures, \**P* < 0.05 and \*\**P* < 0.01 compared to control, one-way ANOVA followed by Bonferroni post hoc test) is shown.

predict the possible interaction of AraC to p75<sup>NTR</sup>. We recently reported that a small molecule (NSC49652) binds to the p75<sup>NTR</sup> TMD and induces cell death both in neurons and cancer cells [33]. Therefore, we speculated that AraC might interact with the TMD of p75<sup>NTR</sup>. Using the p75<sup>NTR</sup> TMD structure that we previously reported [33], our molecular docking data (Fig. 3) suggest that AraC potentially binds to p75<sup>NTR</sup> TMD in a similar region as NSC49652 [33].

Next, we evaluated whether AraC could bind to the TMD of p75<sup>NTR</sup> using an AraTM assay where the bacteria expressed only the TMD of

p75<sup>NTR</sup>. To assess the specificity of AraC binding to p75<sup>NTR</sup> TMD, we used TMD from a different receptor, namely TrkB (Supplementary Fig. 2B). We found that AraC preferentially binds with p75<sup>NTR</sup> TMD (Fig. 4A) although there was some minor binding to TrkB TMD (Supplementary Fig. 2B). After confirming the interaction of AraC to the p75<sup>NTR</sup> TMD, we sought to determine which residues facilitated this interaction. The residues of human p75<sup>NTR</sup> TMD are as follows NLPVYCSILAAVVGLVAYIAFKRW, starting at residue 250. Using a plasmid carrying human p75<sup>NTR</sup> TMD, we mutated isoleucine 252 and valine 254 residues to alanine (I252A and V254A, respectively), located

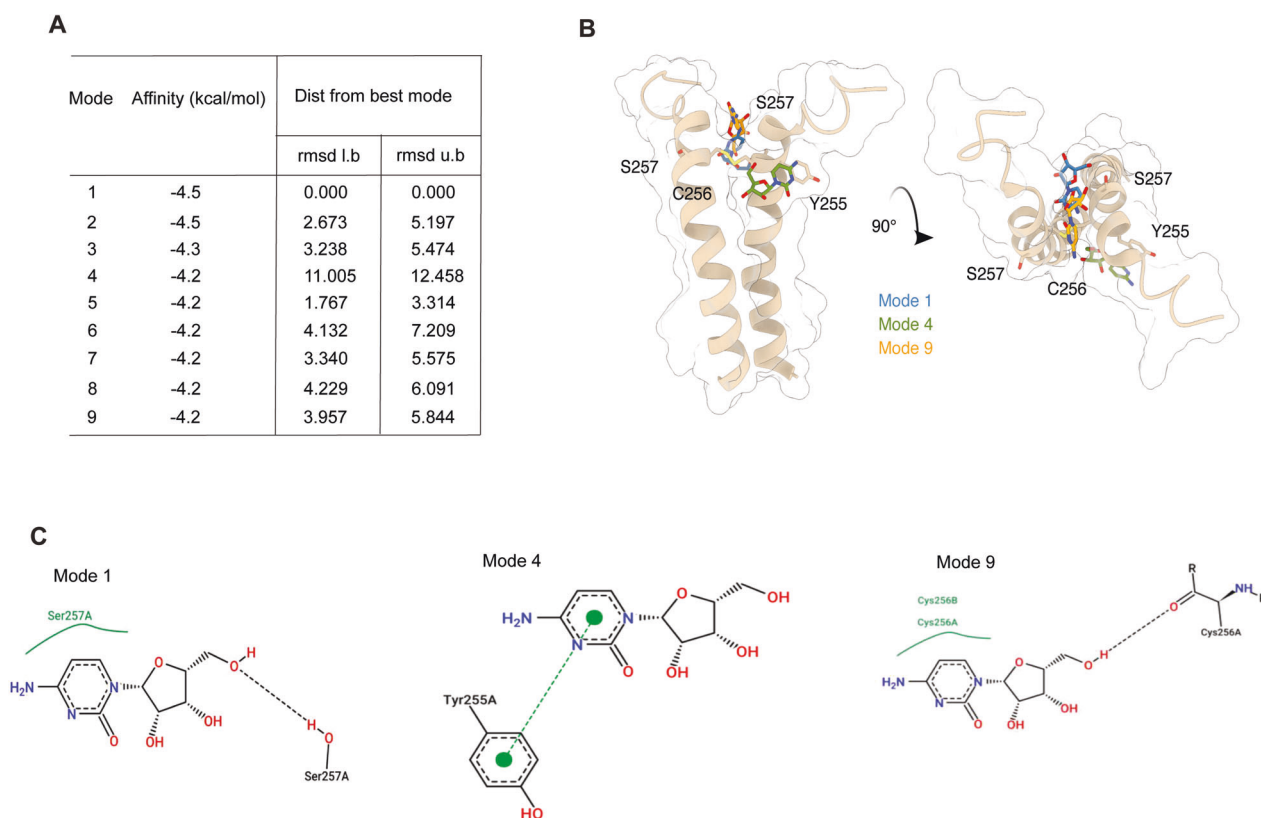


**Fig. 3 Molecular docking results of AraC and p75<sup>NTR</sup> TMD interaction.** **A** Ranked list of potential AraC binding sites and their distance from the highest scoring model. **B** Three principal AraC binding sites were identified and are shown in blue, green and orange stick representation docked onto p75<sup>NTR</sup> TMD. p75<sup>NTR</sup> TMD is shown in tan with a transparent surface, and residues potentially interacting with docked AraC are shown in stick representation. **C** 2D interaction diagrams of the three respective modes.

at the beginning of p75<sup>NTR</sup> TMD. Both bacteria transfected with human wild-type p75<sup>NTR</sup> TMD and p75<sup>NTR</sup> TMD carrying the double mutants, I252A and V254A, responded similarly to AraC treatment (Fig. 4B), suggesting that these two residues are not required for the AraC/p75<sup>NTR</sup> interaction. We then tested human p75<sup>NTR</sup> TMD carrying mutation P253G, where Pro 253 was replaced with glycine. Upon AraC treatment, the bacteria carrying the P253G mutation had a lower percentage of GFP/OD630 compared to bacteria carrying wild-type p75<sup>NTR</sup> TMD (Fig. 4C). This result suggests that the Pro 253 is required for AraC binding to p75<sup>NTR</sup> TMD. We then tested another point mutation, in which the Cys 256 was replaced with alanine (C256A mutant). Similar to P253G, the C256A mutation had a lower percentage of GFP/OD630 compared to wild-type p75<sup>NTR</sup> TMD upon AraC treatment (Fig. 4D). Interestingly, the response of the C256A mutant was already significantly diminished at lower concentration (300  $\mu$ M) of AraC, while the P253G mutant started to show alterations in the response at 500  $\mu$ M of AraC (Fig. 4C, D), suggesting that the Cys 256 is crucial for AraC/p75<sup>NTR</sup> TMD interaction. Taken together, these data demonstrate that Pro 253 and Cys 256 are required for the AraC/p75<sup>NTR</sup> TMD interaction.

We then sought to test whether AraC could interact with full-length p75<sup>NTR</sup> protein. To this end, we used the CETSA which monitors protein–drug interaction by assessing ligand-induced changes in the thermal stability of the protein of interest [55]. First, using protein lysate from 293 T HEK cells that have constitutive expression of p75<sup>NTR</sup>, we generated the p75<sup>NTR</sup> melting curve and found that p75<sup>NTR</sup> starts to melt at 53 °C (Fig. 5A). Then, using the lysate from p75<sup>NTR</sup> expressing HEK cells, we performed isothermal dose response (ITDR)-CETSA to assess the p75<sup>NTR</sup> protein thermal stability at 37 °C and 53 °C after addition of different concentrations of AraC. While the addition of AraC shifted the thermal stability of p75<sup>NTR</sup> in general, the higher concentrations

(100–1000  $\mu$ M) of AraC led to a marked increase in p75<sup>NTR</sup> destabilization at 53 °C (Fig. 5B), suggesting that AraC binding to p75<sup>NTR</sup> result in thermal instability of the protein. Moreover, we found that the addition of 500  $\mu$ M AraC led to p75<sup>NTR</sup> denaturation at lower temperatures starting at 40 °C compared to the control group (Fig. 5C), further supporting AraC-mediated p75<sup>NTR</sup> destabilization. Altogether, these data suggest that AraC interacts with full-length mammalian p75<sup>NTR</sup>.

Next, we sought to confirm that AraC could still bind to p75<sup>NTR</sup> in intact cells using a homo-FRET anisotropy assay. COS-7 cells were transfected with a plasmid expressing a full-length rat p75<sup>NTR</sup>-EGFP\* fusion [42], and 24 h later, the changes in anisotropy levels after treatment with DMSO (control) or AraC were recorded over a certain amount of time. Treatment with AraC induced oscillation of p75<sup>NTR</sup> anisotropy at the cell membrane (Fig. 5D, E), resulting in a positive net change of the integrated peak area over 15 min treatment compared with vehicle (Fig. 5D, F). Interestingly, the frequency of the anisotropy oscillation after AraC treatment was similar to the anisotropy changes above or under the control basal line (DMSO average anisotropy values) (Fig. 5G). Together, these data demonstrate that AraC interacts with p75<sup>NTR</sup>.

### AraC selectively uncouples p75<sup>NTR</sup> from the NF $\kappa$ B signalling pathway

We previously showed that activation of p75<sup>NTR</sup>-dependent nuclear factor kappa-light-chain-enhancer of activated B cells (NF $\kappa$ B) signalling pathway is crucial for the survival of CGNs [51]. Therefore, we evaluated whether AraC treatment induces uncoupling of p75<sup>NTR</sup> from the NF $\kappa$ B signalling pathway. p75<sup>NTR</sup>-mediated activation of the NF $\kappa$ B pathway leads to the phosphorylation and subsequent degradation of I $\kappa$ B $\alpha$  (nuclear factor of kappa light polypeptide gene enhancer in B-cells inhibitor, alpha),

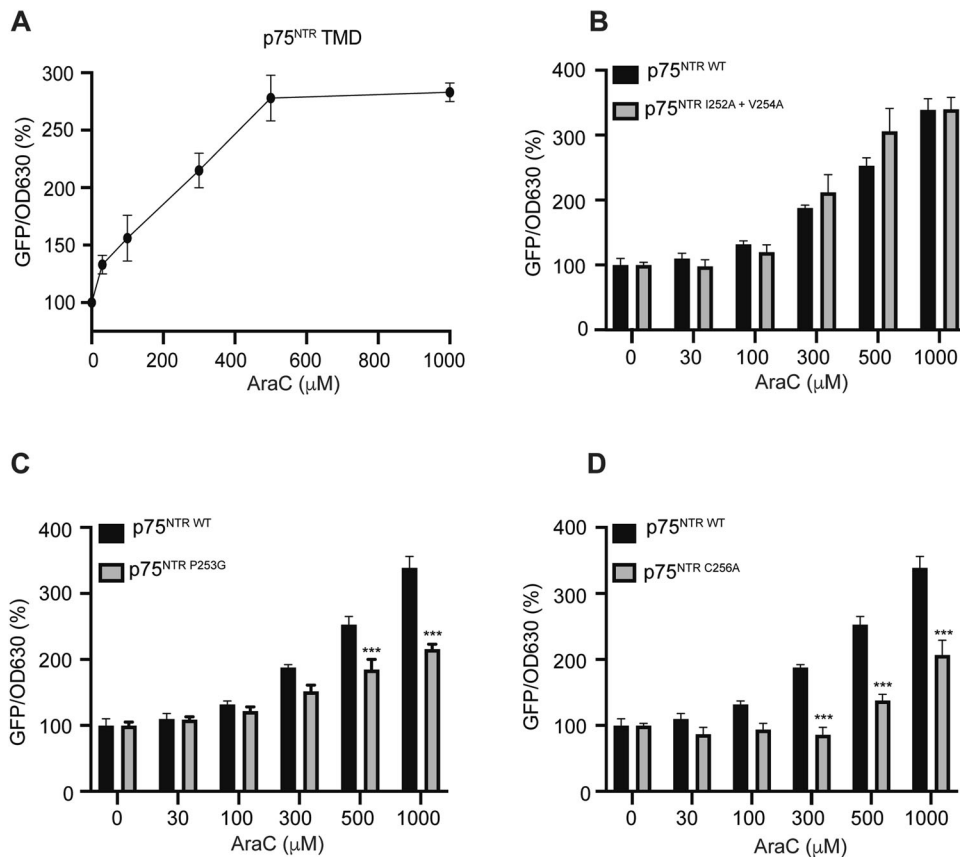


**Fig. 4** AraC requires Pro253 and Cys256 to interact with p75<sup>NTR</sup> TMD. **A** Dose response of AraC in the AraTM assay of p75<sup>NTR</sup>. Results are plotted as means  $\pm$  SD ( $N = 3$ ). **B–D** Comparison of human wild-type p75<sup>NTR</sup> TMD with p75<sup>NTR</sup> TMD with I252A plus V254A (**B**) or P253G (**C**) or C256A (**D**) mutants in the AraTM assay in response to increasing doses of AraC. The GFP over OD630 signal without any drug added was set at 100%. Results are plotted as means  $\pm$  SD ( $N = 3$ ). Significance was calculated using the two-way ANOVA followed by Bonferroni post hoc test where \*\* $p < 0.01$  and \*\*\* $p < 0.001$ .

which does not cover the nuclear localisation signal of the cytosolic P65NFkB anymore leading to its translocation to the nucleus [51, 56]. Neurons treated with AraC for 30 min at 4 DIV showed lower P65NFkB immunoreactivity in the nucleus compared to control (Fig. 6A, B), suggesting that P65NFkB remains bound to I $\kappa$ B $\alpha$  in the cytosol. Therefore, we evaluated the degradation of I $\kappa$ B $\alpha$  in untreated (naïve) cells and after treatment with 500  $\mu$ M AraC. We observed a decrease in I $\kappa$ B $\alpha$  degradation after 30 and 60 min of AraC treatment (Fig. 6C). Since our AraC/p75<sup>NTR</sup> data suggest that C259 is crucial for this interaction (Fig. 4D), we hypothesised that the effect of AraC on neurons lacking this residue will be abrogated. As expected, WT neurons treated with AraC had an accumulation of I $\kappa$ B $\alpha$  in the cytosol, while C256A neurons had a less pronounced I $\kappa$ B $\alpha$  accumulation after AraC treatment (Fig. 6D). Together, these data indicate that the AraC/p75<sup>NTR</sup> TMD interaction leads to uncoupling of p75<sup>NTR</sup> from the NF $\kappa$ B signalling pathway resulting in the accumulation of I $\kappa$ B $\alpha$  in the cytosol and less translocation of P65NFkB to the nucleus.

Finally, we evaluated apoptotic activity in wild-type and C259A neurons after 24 h treatment with AraC. As expected from our previous results, treatment of wild-type CGNs with AraC increased the percentage of cleaved caspase 3 positive cells in the cultures (Fig. 6E, F). On the other hand, although C259A CGNs treated with AraC also showed an increase in the number of cleaved caspase 3 positive neurons, the number of apoptotic cells was 50% lower than in the WT neurons (Fig. 6E, F). These results indicate that C259 is involved in the AraC/p75<sup>NTR</sup> TMD interaction, but other residues are necessary since that mutation does not completely block the apoptotic effect induced by the drug.

#### AraC/p75<sup>NTR</sup> interaction does not affect p75<sup>NTR</sup>-dependent TrkB and RhoA signalling

Next, we dissected the signalling mechanism that AraC/p75<sup>NTR</sup> employs to elicit cell death of mature CGNs. p75<sup>NTR</sup> is known to engage several signalling pathways by interacting with other receptors and recruiting a number of adaptor proteins to its death domain, which lacks enzymatic activity [23, 50, 51, 56–60]. Moreover, p75<sup>NTR</sup> has been suggested to increase the affinity of neurotrophins for Trk receptors [61–63]. To dissect the signalling mechanism that AraC/p75<sup>NTR</sup> employs to elicit cell death of mature CGNs, we first evaluated whether the binding of AraC to p75<sup>NTR</sup> TMD interferes with the activation of the survival of the TrkB signalling pathway that is indispensable for the survival of neurons [64]. Upon activation by neurotrophins or pharmacological drugs, TrkB is phosphorylated on several residues, including tyrosine 515 [64, 65]. Phosphorylation of tyrosine 515 regulates protein kinase B (AKT), which plays an important role in cell survival [66]. We, therefore, first evaluated the expression of TrkB in 4 DIV CGNs (Supplementary Fig. 2A) and the phosphorylation of TrkB, particularly on tyrosine 515, observing no changes upon AraC treatment (Supplementary Fig. 2C, D). This result suggests that the binding of AraC to p75<sup>NTR</sup> TMD does not interfere with p75<sup>NTR</sup>-dependent TrkB activity. We then asked whether the AraC/p75<sup>NTR</sup> interaction affects the signalling pathways (RhoA, JNK and NF $\kappa$ B pathways) that are downstream to p75<sup>NTR</sup> [23, 60]. We assessed the AraC/p75<sup>NTR</sup> interaction might modulate p75<sup>NTR</sup>-dependent RhoA activity in these neurons. However, CGNs treated at 4 DIV with AraC did not show any alteration in the levels of RhoA activity (Supplementary Fig. 2F).

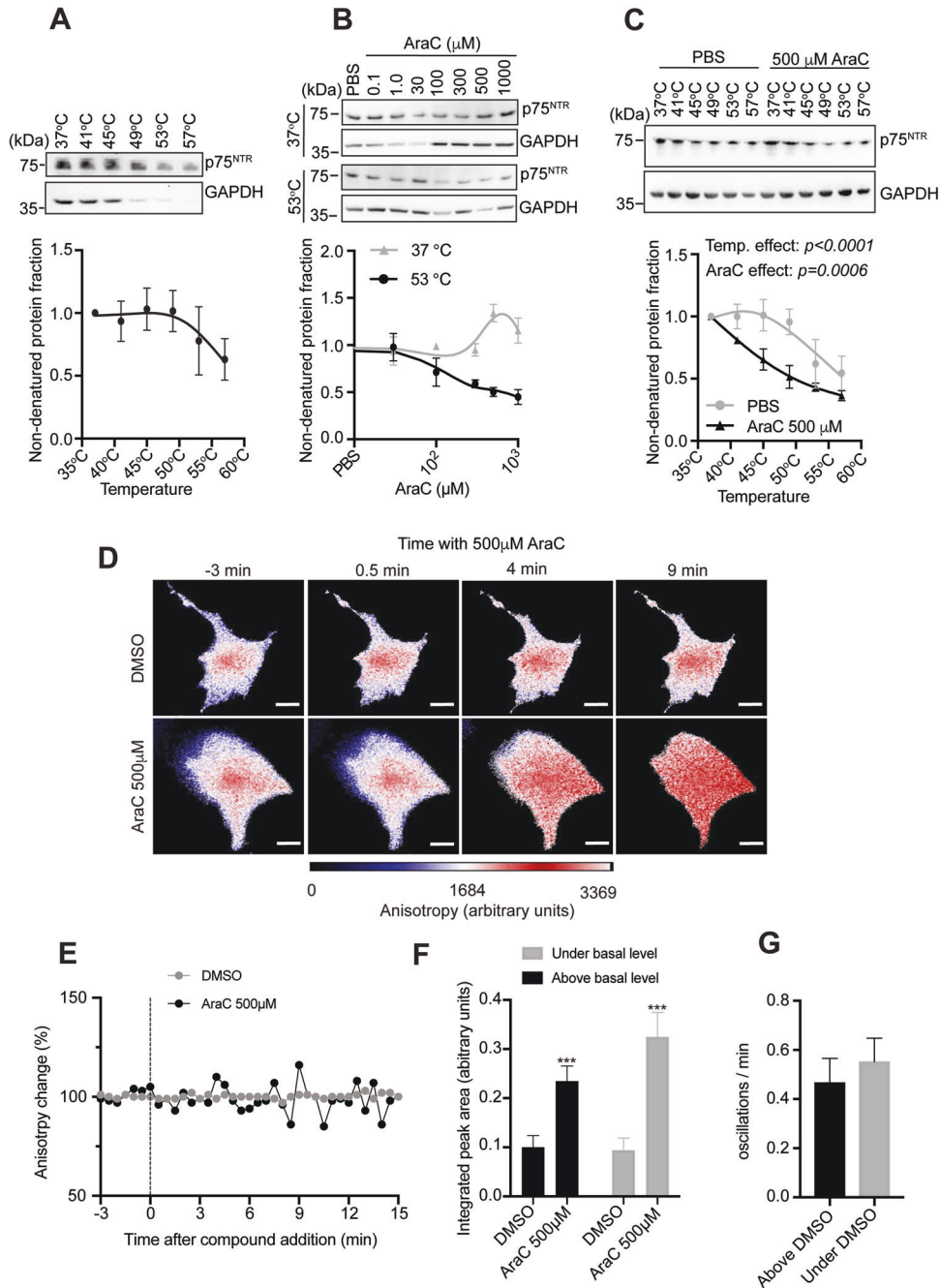


**Fig. 5** AraC changes the properties of the p75<sup>NTR</sup> protein. **A** Representative immunoblot probed for p75<sup>NTR</sup> and GAPDH and quantification of CETSA for p75<sup>NTR</sup> protein response to different temperatures. **B** Representative immunoblot probed for p75<sup>NTR</sup> and GAPDH and quantification of p75<sup>NTR</sup> CETSA for AraC dose-response on protein lysate extracted from HEK293 cells constitutively overexpressing p75<sup>NTR</sup>. The lysate was heated to 37 °C and 53 °C. **C** Representative immunoblot probed for p75<sup>NTR</sup> and GAPDH and quantification of p75<sup>NTR</sup> CETSA for p75<sup>NTR</sup> response to temperature after treatment with either PBS (vehicle) or 500 μM AraC. Mean ± s.e.m. of data from 3 to 6 separate cultures is shown for p75<sup>NTR</sup>. **D** Live cell homo-FRET anisotropy of p75<sup>NTR</sup> in COS-7 cells in response to AraC. Shown are representative time-lapse images before (-3 min) and after (0.5, 4 and 9 min) addition of 500 μM AraC or DMSO (control). Scale bars, 5 μm. **E** Live cell homo-FRET anisotropy of p75<sup>NTR</sup> in COS-7 cells in response to AraC. Shown are representative traces of average anisotropy change after the addition of AraC (500 μM at 0 min) or vehicle in cells expressing wild-type rat p75<sup>NTR</sup>. **F** Integrated peak area of live cell homo-FRET anisotropy of p75<sup>NTR</sup> in COS-7 cells in response to AraC (considering the area under and above  $y = 1$ ). Results are plotted as means ± SD ( $N = 7$ ). \*\*\* $P < 0.001$ ; Student *t*-test. **G** Oscillations/min of live cell homo-FRET anisotropy of p75<sup>NTR</sup> in COS7 cells in response to AraC (considering the vehicle oscillations as threshold). Results are plotted as means ± SD ( $N = 7$ ).

#### AraC/p75<sup>NTR</sup>- mediated inactivation of NFκB pathway exacerbates neurodegeneration by activating cell death/JNK pathway

We previously reported that uncoupling of p75<sup>NTR</sup> from NFκB leads to cell death by activation of the JNK pathway [51]. In the

absence of RIP2, an adaptor protein linking p75<sup>NTR</sup> to the NFκB pathway, p75<sup>NTR</sup> binds to TRAF6, another adaptor protein that links p75<sup>NTR</sup> to the JNK apoptotic pathway. For this reason, we asked whether AraC-mediated inactivation of the NFκB pathway could lead to the activation of the JNK pathway, exacerbating



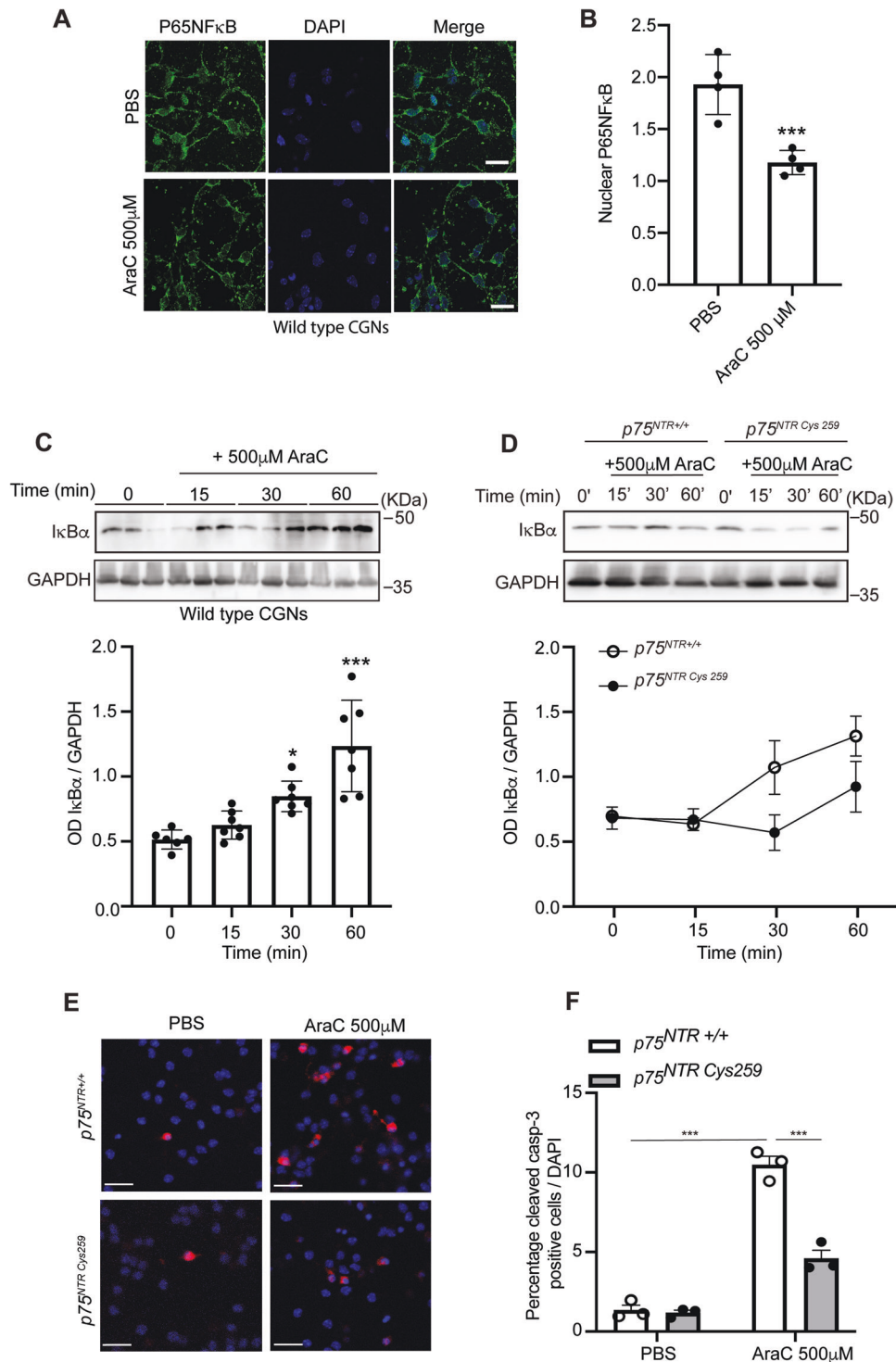


**Fig. 6** AraC selectively uncouples  $p75^{\text{NTR}}$  from  $\text{NF}\kappa\text{B}$  signalling pathway. **A** Representative images of wild-type P7 CGNs cultured for 4 days, treated with either PBS (control) or 500  $\mu\text{M}$  AraC for 60 min, fixed, stained for P65NF $\kappa\text{B}$  (green) and counterstained with DAPI (blue). Scale bar, 50  $\mu\text{m}$ . **B** Quantification of the P65NF $\kappa\text{B}$  nuclear translocation in PBS (control) or neurons treated with 500  $\mu\text{M}$  AraC for 60 min. Mean  $\pm$  s.e.m. of data from four separate cultures, \*\*\* $P < 0.001$  compared to control, unpaired Student  $t$ -test) is shown. **C** Representative western blots probed with I $\kappa\text{B}\alpha$  and GAPDH of lysate of wild-type P7 CGNs grown for 4 days prior to stimulation with 500  $\mu\text{M}$  AraC for 15, 30 or 60 min. **D** Quantification of I $\kappa\text{B}\alpha$  degradation in the total lysate of untreated wild-type P7 CGNs or neurons treated with 500  $\mu\text{M}$  AraC for 15, 30 or 60 min. Mean  $\pm$  sem of densitometry from 6 experiments (\*\*\* $P < 0.001$ ; one-way ANOVA followed by Bonferroni test) is shown. **E** Representative images of wild type or C259A mutant P7 CGNs cultured for 4 DIV that were either treated with PBS (control) or 500  $\mu\text{M}$  AraC for 24 h and stained for cleaved caspase 3 (red) and counterstained with DAPI (blue). Scale bars, 50  $\mu\text{m}$ . **F** Quantification of percentage cleaved caspase 3 positive neurons wild type or C259A mutant CGNs treated with either PBS (control) or AraC (500  $\mu\text{M}$ ) for 24 h (total of 60 images per condition were counted). Mean  $\pm$  s.e.m. of data from four separate cultures, \*\*\* $P < 0.001$  compared to control, one-way ANOVA followed by Bonferroni post hoc test) is shown.

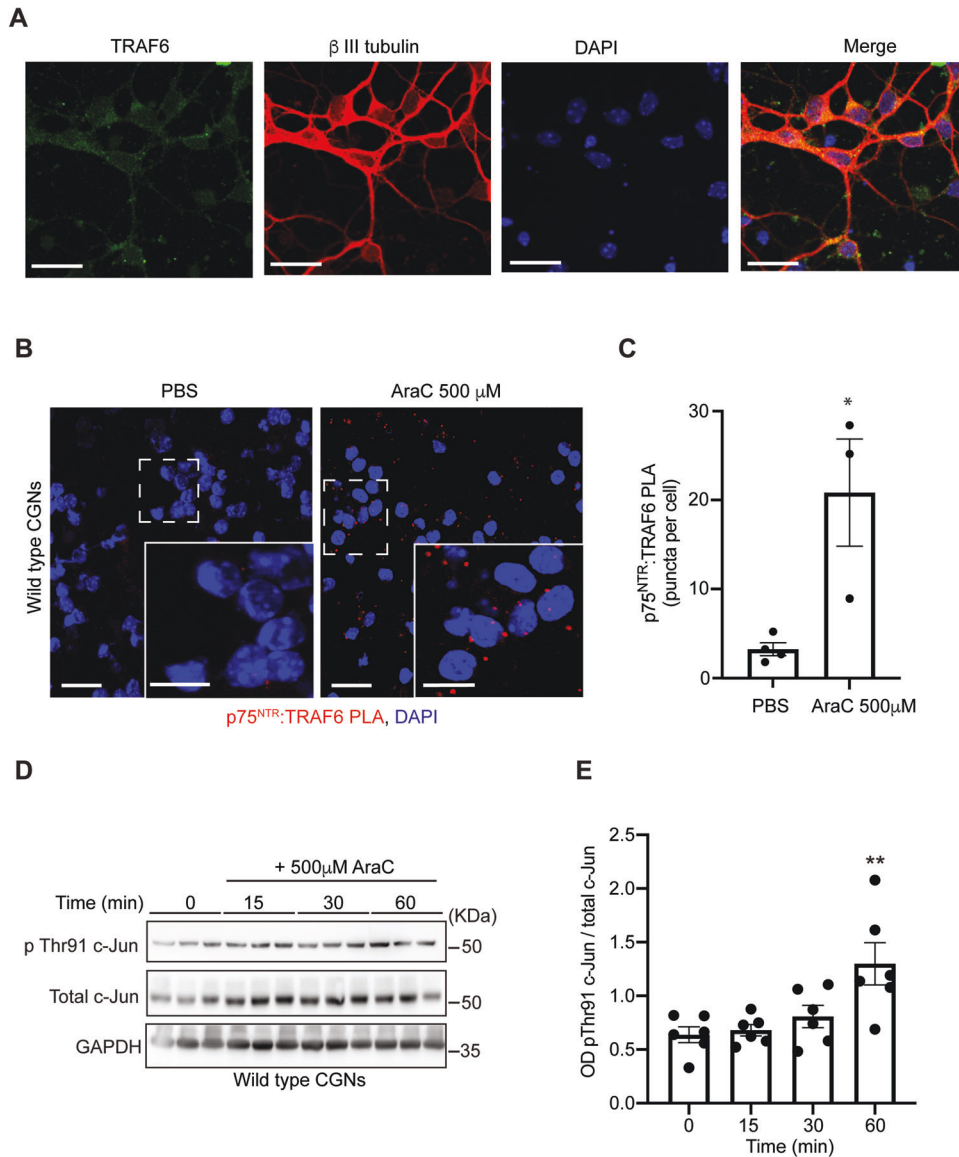


**Fig. 7** AraC/p75<sup>NTR</sup>-mediated inactivation of NFκB pathway exacerbates neuronal death by activating the JNK pathway. **A** Representative micrographs of wild-type P7 CGNs cultured for 4DIV and double stained with anti-TRAF6 together with anti-β III tubulin and counterstained with DAPI. Scale bars, 50 μm. **B** Micrographs of p75<sup>NTR</sup>:TRAF6 PLA (red) in CGNs treated with either PBS (control) or 500 μM AraC for 10 min. Images were selected from 25 images per condition from 3 to 4 separate experiments. Scale bar, 20 μm. **C** Quantification of p75<sup>NTR</sup>:TRAF6 PLA puncta in CGNs treated with either PBS (control) or 500 μM AraC for 10 min. Mean ± sem of data from 3 experiments (\**P* < 0.05; unpaired Student *t*-test) is shown. **D** Representative western blots probed with phospho-c-Jun (Thr91), total c-Jun and GAPDH of lysates of wild type P7 CGNs grown for 4 days prior to 15-, 30- or 60-min treatment with 500 μM AraC. **E** Quantification of c-Jun (Thr91) phosphorylation of total lysate of untreated wild-type P7 CGNs or neurons treated with 500 μM for 15, 30 and 60 min. Mean ± sem of densitometry from 4 experiments (\**P* < 0.05; one-way ANOVA followed by Bonferroni test) is shown.

neuronal apoptosis. First, we confirmed the expression of TRAF6 in 4 DIV CGNs (Fig. 7A). Next, the recruitment of TRAF6 to the intracellular domain of p75<sup>NTR</sup> after AraC treatment was assessed in the CGNs cultures at 4 DIV by PLA. We detected an increase in p75<sup>NTR</sup>:TRAF6 PLA puncta (Fig. 7B, C) that suggested that AraC alters the conformation of p75<sup>NTR</sup>, favouring the binding of TRAF6. Then, we evaluated the activation of the JNK apoptotic pathway by assessing the phosphorylation of c-Jun on threonine 91 (Thr91), which has been linked to cell death in CGNs [67]. Indeed, the interaction of AraC with wild-type p75<sup>NTR</sup> increased the phosphorylation of c-Jun on Threonine 91 residue (Fig. 7D, E). Altogether, these data indicate that treatment of CGNs with a high concentration of AraC inhibits the NFκB survival pathway and potentiates the JNK apoptotic pathway.

## DISCUSSION

AraC has successfully been used as a chemotherapeutic for decades, being the most effective chemotherapy for the treatment of several cancers, including AML, acute lymphatic leukaemia (ALL) and non-Hodgkin's lymphoma [1–4]. Similar to other chemotherapy treatments, AraC has several side effects, including neurotoxicity [3, 6, 7]. Interestingly, AraC-induced neurotoxicity is age-dependent; the older the patient is, the more severe the neurotoxicity, as older patients often require higher doses of AraC treatment [11]. In the current study, we show that high doses of AraC induce apoptosis in mature cerebellar neurons. These results are in agreement with observations made in adult cancer patients under the HIDAC treatment regime, who developed cerebellar atrophy and shrinkage leading to impaired cerebellar function that,

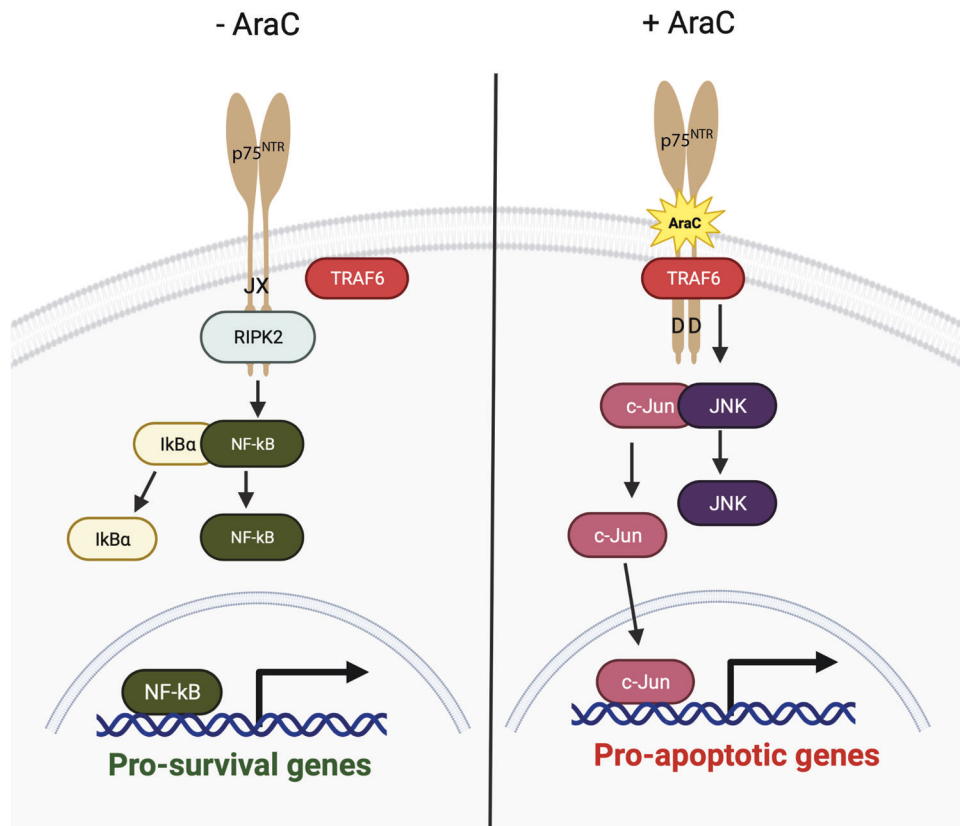


**Fig. 8 Molecular mechanism of AraC/p75<sup>NTR</sup> interaction in the regulation of neuronal death.** This schematic diagram depicts p75<sup>NTR</sup> signalling in healthy mature neurons and when AraC interacts with p75<sup>NTR</sup>. Upon AraC binding to p75<sup>NTR</sup>, RIPK2 is dislodged from the death domain (DD), allowing the exposure of the juxta membrane (JX), where TRAF6 binds. The binding of TRAF6 to p75<sup>NTR</sup> activates the JNK pathways that lead to the translocation of c-Jun to the nucleus and transcription of pro-apoptotic genes. Figure produced in BioRender.

in some cases, was permanent [11, 44]. As expected, the mature CGNs in vitro express the death receptor, p75<sup>NTR</sup>. Although it has been suggested that p75<sup>NTR</sup> expression is markedly reduced in adult neurons [17], the expression of this receptor is not completely abrogated in the adult cerebellum [19, 51]. Moreover, recent single-cell RNA sequencing data confirms the expression of p75<sup>NTR</sup> in the majority of adult cerebellar neurons [68]. Interestingly, acute leukaemia patients show expression of p75<sup>NTR</sup> both on malignant and normal lymphocytes, as well as an increase in expression of p75<sup>NTR</sup> in serum, bone marrow and peripheral blood cells [24, 25]. Moreover, our data show that AraC treatment increases the expression of p75<sup>NTR</sup> in mature CGNs. Therefore, it is plausible that there is also an increase of p75<sup>NTR</sup> in the cerebellum of leukaemia patients making them more susceptible to AraC-mediated neurodegeneration through p75<sup>NTR</sup>. In agreement with this, our data demonstrate that deletion of p75<sup>NTR</sup> in mature CGNs prevented AraC-induced apoptosis.

p75<sup>NTR</sup> facilitates different effects in CGNs, including axonal degeneration, cell survival, apoptosis and growth inhibition [22, 23]. These effects are achieved due to p75<sup>NTR</sup>'s capability to couple different signalling pathways, including NFκB, JNK/caspase and RhoDGI/RhoA pathways in these neurons [23, 60]. This raises the question as to why the interaction of AraC to p75<sup>NTR</sup> induces neurite degeneration and cell death and not survival or growth inhibition in mature CGNs. It is noteworthy that the outcome of AraC interaction with p75<sup>NTR</sup> depends on the availability of adaptor proteins (TRAF6, RIP2 and RhoA) and the signalling pathway that will be engaged.

We find that AraC binds to the TMD of p75<sup>NTR</sup>. Recent findings have demonstrated that a couple of small molecules bind to the TMD of certain receptors; for instance, SB394725 binds TMD of the

thrombopoietin receptor [69], and NCS49652, a compound that binds to the TMD of p75<sup>NTR</sup> [33]. The binding of AraC to p75<sup>NTR</sup> TMD leads to anisotropy oscillations that are different to those induced by the binding of NCS49652 [33], suggesting that the two compounds bind to different regions of the p75<sup>NTR</sup> TMD. In fact, while NCS49652 binds to Ile252, Pro253, Val 254, Cys256, and serine (Ser) 257 [33], our data suggest that Cys256 and Pro253 contribute to AraC/p75<sup>NTR</sup> TMD interaction. We suggest that this specificity to these two residues could be the reason why AraC does not bind to other members of the TNF superfamily that p75<sup>NTR</sup> belongs to [70, 71].

Interestingly, the interaction of AraC to Cys256 and Pro253 residues in p75<sup>NTR</sup> TMD enables AraC to specifically uncouple p75<sup>NTR</sup> from the NFκB pathway and not any other p75<sup>NTR</sup>-dependent pathway. We previously reported that uncoupling of p75<sup>NTR</sup> from the NFκB pathway leads to apoptosis of CGNs during cerebellar development [51]. Moreover, we showed that in the absence of RIP2, p75<sup>NTR</sup> recruits TRAF6, which couples the receptor to the JNK pathway, leading to an increase in the apoptotic activity of CGNs [51]. Although the wild-type neurons in the current study express both RIP2 and TRAF6, we speculated that the binding of AraC to p75<sup>NTR</sup> TMD changes the conformation of p75<sup>NTR</sup>, hindering the recruitment of RIP2 to p75<sup>NTR</sup> death domain. This new conformation favours the binding of TRAF6 to p75<sup>NTR</sup>, inducing the apoptotic activity of p75<sup>NTR</sup> observed in these neurons. Indeed, our data show that treatment of mature CGNs with AraC leads to increased p75<sup>NTR</sup>:TRAF6 interaction rendering its specificity of activating the TRAF6/JNK cell death pathway.

Although the current work has focused on the effect of AraC on mature CGNs, we speculate that mature neurons in other brain regions that express p75<sup>NTR</sup> could also be affected by this treatment. Interestingly, AraC-treated patients also exhibit

somnolence and drowsiness [72, 73], reinforcing the notion that this drug could alter the function of other brain regions besides the cerebellum. Intriguingly, one brain region that expresses p75<sup>NTR</sup> in abundance in the adult brain is the basal forebrain [18], which has been implicated in the homeostatic regulation of sleep [74–76]. It is, therefore, plausible that the somnolence and drowsiness phenotype observed in patients on HIDAC is a result of AraC/p75<sup>NTR</sup>-mediated neurite degeneration and cell death of the neurons in the basal forebrain.

In conclusion, our data show that p75<sup>NTR</sup> facilitates AraC-induced cell death of mature CGNs by uncoupling p75<sup>NTR</sup> from NFκB pathway and exacerbating cell death/JNK pathway, contributing to cerebellar degeneration (Fig. 8). Our data elucidates the molecular mechanisms of AraC-mediated neurite degeneration and cell death of mature neurons, providing a new molecular target for developing treatments to counteract the side effects of AraC in the CNS.

## DATA AVAILABILITY

All the data used and analysed for this study are available from the corresponding author upon reasonable request.

## REFERENCES

- Cole N, Gibson BE. High-dose cytosine arabinoside in the treatment of acute myeloid leukaemia. *Blood Rev.* 1997;11:39–45.
- Buyukasik Y, Acar K, Kelkitli E, Uz B, Serefhanoglu S, Ozdemir E, et al. Hyper-CVAD regimen in routine management of adult acute lymphoblastic leukemia: a retrospective multicenter study. *Acta Haematol.* 2013;130:199–205.
- Herzig RH, Hines JD, Herzig GP, Wolff SN, Cassileth PA, Lazarus HM, et al. Cerebellar toxicity with high-dose cytosine arabinoside. *J Clin Oncol.* 1987;5:927–32.
- Press OW, Livingston R, Mortimer J, Collins C, Appelbaum F. Treatment of relapsed non-hodgkin's lymphomas with dexamethasone, high-dose cytarabine, and cisplatin before marrow transplantation. *J Clin Oncol.* 1991;9:423–31.
- Momparler RL. Optimization of cytarabine (ARA-C) therapy for acute myeloid leukemia. *Exp Hematol Oncol.* 2013;2:20.
- Lazarus HM, Herzig RH, Fishman DJ, Herzig GP, Phillips GL, Roessmann U. Central nervous system toxicity of high-dose systemic cytosine arabinoside. *Cancer* 1981;48:2577–82.
- Grossman L, Baker MA, Sutton DMC, Deck JHN. Central nervous system toxicity of high-dose cytosine arabinoside. *Med Pediatr Oncol.* 1983;11:246–50.
- Dessi F, Pollard H, Moreau J, Ben-Ari Y, Charriaud-Marlangue C. Cytosine arabinoside induces apoptosis in cerebellar neurons in culture. *J Neurochem.* 1995;64:1980–7.
- Courtney MJ. The mechanism of Ara-C-induced apoptosis of differentiating cerebellar granule neurons. *Eur J Neurosci.* 1999;3:1073–84.
- Benger A, Browman GP, Walker IR, Preisler HD. Clinical evidence of a cumulative effect of high-dose cytarabine on the cerebellum in patients with acute leukemia: a leukemia intergroup report. *Cancer Treat Rep.* 1985;69:240–1.
- Gottlieb D, Bradstock K, Koutts J, Robertson T, Lee C, Castaldi P. The neurotoxicity of high-dose cytosine arabinoside is age-related. *Cancer.* 1987;60:1439–41.
- Eriksson PS, Perfilieva E, Björk-Eriksson T, Alborn AM, Nordborg C, Peterson DA, et al. Neurogenesis in the adult human hippocampus. *Nat Med.* 1998;4:1313–7.
- Bergmann O, Liebl J, Bernard S, Alkass K, Yeung MSY, Steier P, et al. The age of olfactory bulb neurons in humans. *Neuron* 2012;74:634–9.
- Kufe DW, Major PP. Studies on the mechanism of action of cytosine arabinoside. *Med Pediatr Oncol.* 1982;10:49–67.
- Major PP, Egan EM, Herrick DJ, Kufe DW. Effect of ara-C incorporation on deoxyribonucleic acid synthesis in cells. *Biochem Pharmacol.* 1982;31:2937–40.
- Kufe DW, Griffin JD, Spriggs DR. Cellular and clinical pharmacology of low-dose ara-C. *Semin Oncol.* 1985;12:200–7.
- Meeker R, Williams K. Dynamic nature of the p75 neurotrophin receptor in response to injury and disease. *J Neuroimmune Pharmacol.* 2014;9:615–28.
- Pioro EP, Cuello AC. Distribution of nerve growth factor receptor-like immunoreactivity in the adult rat central nervous system. Effect of colchicine and correlation with the cholinergic system-II. Brainstem, cerebellum and spinal cord. *Neuroscience.* 1990;34:89–110.
- Ernfors P, Hallbook F, Ebendal T, Shooter EM, Radeke MJ, Misko TP, et al. Developmental and regional expression of β-nerve growth factor receptor mRNA in the chick and rat. *Neuron* 1988;1:983–96.
- Dechant G, Barde YA. The neurotrophin receptor p75<sup>NTR</sup>: novel functions and implications for diseases of the nervous system. *Nat Neurosci.* 2002;5:1131–6.
- Chao MY, Rajagopal R, Lee FS. Neurotrophin signalling in health and disease. *Clin Sci.* 2006;110:167–73.
- Ibáñez CF, Simi A. P75 neurotrophin receptor signaling in nervous system injury and degeneration: paradox and opportunity. *Trends Neurosci.* 2012;35:431–40.
- Kraemer BR, Yoon SO, Carter BD. The biological functions and signaling mechanisms of the p75 neurotrophin receptor. *Handb Exp Pharm.* 2014;220:121–64.
- Beutel G, Meyer J, Ma L, Yin S, Eder M, Von Neuhoff N, et al. Expression of the p75 neurotrophin receptor in acute leukaemia. *Br J Haematol.* 2005;131:67–70.
- Molica S, Vitelli G, Levato D, Crispino G, Dell'Olio M, Dattilo A, et al. CD27 in B-cell chronic lymphocytic leukemia. Cellular expression, serum release and correlation with other soluble molecules belonging to nerve growth factor receptors (NGFr) superfamily. *Haematologica.* 1998;83:398–402.
- Lee KF, Li E, Huber LJ, Landis SC, Sharpe AH, Chao MV, et al. Targeted mutation of the gene encoding the low affinity NGF receptor p75 leads to deficits in the peripheral sensory nervous system. *Cell* 1992;69:737–49.
- Tanaka K, Kelly CE, Goh KY, Lim KB, Ibáñez CF. Death domain signaling by disulfide-linked dimers of the p75 neurotrophin receptor mediates neuronal death in the CNS. *J Neurosci.* 2016;36:5587–95.
- Josting A, Rudolph C, Reiser M, Mapara M, Sieber M, Kirchner HH, et al. Time-intensified dexamethasone/cisplatin/cytarabine: An effective salvage therapy with low toxicity in patients with relapsed and refractory Hodgkin's disease. *Ann Oncol.* 2002;13:1628–35.
- Weiss MA, Aliff TB, Tallman MS, Frankel SR, Kalaycio ME, Maslak PG, et al. A single, high dose of idarubicin combined with cytarabine as induction therapy for adult patients with recurrent or refractory acute lymphoblastic leukemia. *Cancer.* 2002;95:581–7.
- Velasquez W, Cabanillas F, Salvador P, McLaughlin P, Fridrik M, Tucker S, et al. Effective salvage therapy for lymphoma with cisplatin in combination with high-dose Ara-C and dexamethasone (DHAP). *Blood.* 1988;71:117–12.
- Di Francia R, Crisci S, De Monaco A, Caferio C, Re A, Iaccarino G, et al. Response and toxicity to cytarabine therapy in leukemia and lymphoma: From dose puzzle to pharmacogenomic biomarkers. *Cancers.* 2021;13:966.
- Kraemer BR, Snow JP, Vollbrecht P, Pathak A, Valentine WM, Deutch AY, et al. A role for the p75 neurotrophin receptor in axonal degeneration and apoptosis induced by oxidative stress. *J Biol Chem.* 2014;289:21205–16.
- Goh ETH, Lin Z, Ahn BY, Lopes-Rodrigues V, Dang NH, Salim S, et al. A small molecule targeting the transmembrane domain of death receptor p75 NTR induces melanoma cell death and reduces tumor growth. *Cell Chem Biol.* 2018;25:1485–94.e5.
- Morris GM, Huey R, Lindstrom W, Sanner MF, Belew RK, Goodsell DS, et al. AutoDock4 and AutoDockTools4: automated docking with selective receptor flexibility. *J Comput Chem.* 2009;30:2785–91.
- Trott O, Olson AJ. AutoDock Vina: Improving the speed and accuracy of docking with a new scoring function, efficient optimization, and multithreading. *J Comput Chem.* 2009;31:455–61.
- Schöning-Stierand K, Diedrich K, Fährrolfes R, Flachsenberg F, Meyder A, Nittinger E, et al. ProteinsPlus: interactive analysis of protein–ligand binding interfaces. *Nucleic Acids Res.* 2020;48:W48–W53.
- Stierand K, Maaß PC, Rarey M. Rarey M Molecular complexes at a glance: automated generation of two-dimensional complex diagrams. *Bioinformatics.* 2006;22:1710–6.
- Pettersen EF, Goddard TD, Huang CC, Meng EC, Couch GS, Croll TI, et al. UCSF ChimeraX: structure visualization for researchers, educators, and developers. *Protein Sci.* 2021;30:70–82.
- Su PC, Berger BW. Identifying key juxtamembrane interactions in cell membranes using AraC-based transcriptional reporter assay (AraTM). *J Biol Chem.* 2012;287:31515–26.
- Su PC, Berger BW. A novel assay for assessing juxtamembrane and transmembrane domain interactions important for receptor heterodimerization. *J Mol Biol.* 2013;425:4652–8.
- Park DI, Novak B, Yan Y, Kaya ME, Turck CW. Paroxetine binding and activation of phosphofruktokinase implicates energy metabolism in antidepressant mode of action. *J Psychiatr Res.* 2020;129:8–14.
- Vilar M, Charalampopoulos I, Kenchappa RS, Simi A, Karaca E, Reversi A, et al. Activation of the p75 neurotrophin receptor through conformational rearrangement of disulfide-linked receptor dimers. *Neuron* 2009;62:72–83.
- Lin Z, Tann JY, Goh ETH, Kelly C, Lim KB, Gao JF, et al. Structural basis of death domain signaling in the p75 neurotrophin receptor. *Elife.* 2015;4:e11692.
- Nowacki P, Dolińska D, Honczarenko K, Zyluk B. Atrophy of the granular layer of the cerebellar cortex in patients with nonlymphoblastic leukemia treated with cytosine arabinoside. *Neurol Neurochir Pol.* 1992;26:482–9.
- Enokido Y, Araki T, Aizawa S, Hatanaka H. p53 involves cytosine arabinoside-induced apoptosis in cultured cerebellar granule neurons. *Neurosci Lett.* 1996;203:1–4.

46. Koros C, Kitraki E. Effect of cytosine arabinoside on cerebellar neurofilaments during development: a sexual dimorphism. *Toxicol Rep.* 2014;1:650–7.
47. Manzini MC, Ward MS, Zhang Q, Lieberman MD, Mason CA. The stop signal revised: Immature cerebellar granule neurons in the external germinal layer arrest pontine mossy fiber growth. *J Neurosci.* 2006;26:6040–51.
48. Yoon SO, Casaccia-Bonnel P, Carter B, Chao MV. Competitive signaling between TrkA and p75 nerve growth factor receptors determines cell survival. *J Neurosci.* 1998;18:3273–81.
49. Friedman WJ. Neurotrophins induce death of hippocampal neurons via the p75 receptor. *J Neurosci.* 2000;20:6340–6.
50. Wicovsky A, Müller N, Daryab N, Marienfeld R, Kneitz C, Kavuri S, et al. Sustained JNK activation in response to tumor necrosis factor is mediated by caspases in a cell type-specific manner. *J Biol Chem.* 2007;282:2174–83.
51. Kisiswa L, Fernández-Suárez D, Sergaki MC, Ibáñez CF. RIP2 gates TRAF6 interaction with death receptor p75NTR to regulate cerebellar granule neuron survival. *Cell Rep.* 2018;24:1013–24.
52. Fernández-Suárez D, Krapacher FA, Andersson A, Ibáñez CF, Kisiswa L. MAG induces apoptosis in cerebellar granule neurons through p75NTR demarcating granule layer/white matter boundary. *Cell Death Dis.* 2019;10:732.
53. Zagrebelsky M, Holz A, Dechant G, Barde YA, Bonhoeffer T, Korte M. The p75 neurotrophin receptor negatively modulates dendrite complexity and spine density in hippocampal neurons. *J Neurosci.* 2005;25:9989–99.
54. Roux PP, Barker PA. Neurotrophin signaling through the p75 neurotrophin receptor. *Prog Neurobiol.* 2002;67:203–33.
55. Molina DM, Jafari R, Ignatushchenko M, Seki T, Larsson EA, Dan C, et al. Monitoring drug target engagement in cells and tissues using the cellular thermal shift assay. *Science.* 2013;341:84–7.
56. Vicario A, Kisiswa L, Tann JY, Kelly CE, Ibanez CF. Neuron-type-specific signaling by the p75NTR death receptor is regulated by differential proteolytic cleavage. *J Cell Sci.* 2015;128:1507–17.
57. Carter BD, Kaltschmidt C, Kaltschmidt B, Offenhäuser N, Böhm-Matthaei R, Baeuerle PA, et al. Selective activation of NF- $\kappa$ B by nerve growth factor through the neurotrophin receptor p75. *Science.* 1996;272:542–5.
58. Khursigara G, Bertin J, Yano H, Moffett H, DiStefano PS, Chao MV. A prosurvival function for the p75 receptor death domain mediated via the caspase recruitment domain receptor-interacting protein 2. *J Neurosci.* 2001;21:5854–63.
59. McCarthy JV, Ni J, Dixit VM. RIP2 is a novel NF- $\kappa$ B-activating and cell death-inducing kinase. *J Biol Chem.* 1998;273:16968–75.
60. Gehler S, Gallo G, Veien E, Letourneau PC. p75 neurotrophin receptor signaling regulates growth cone filopodial dynamics through modulating RhoA activity. *J Neurosci.* 2004;24:4363–72.
61. Hempstead BL, Martin-Zanca D, Kaplan DR, Parada LF, Chao MV. High-affinity NGF binding requires coexpression of the trk proto-oncogene and the low-affinity NGF receptor. *Nature.* 1991;350:678–83.
62. Clary DO, Reichardt LF. An alternatively spliced form of the nerve growth factor receptor TrkA confers an enhanced response to neurotrophin 3. *Proc Natl Acad Sci USA.* 1994;91:11133–7.
63. Zanin JP, Montroull LE, Volosin M, Friedman WJ. The p75 neurotrophin receptor facilitates TrkB signaling and function in rat hippocampal neurons. *Front Cell Neurosci.* 2019;13:485.
64. Huang EJ, Reichardt LF. Neurotrophins: roles in neuronal development and function. *Annu Rev Neurosci.* 2001;24:677–736.
65. Rantamäki T. TrkB neurotrophin receptor at the core of antidepressant effects, but how? *Cell Tissue Res.* 2019;377:115–124.
66. Kim AH, Khursigara G, Sun X, Franke TF, Chao MV. Akt phosphorylates and negatively regulates apoptosis signal-regulating kinase 1. *Mol Cell Biol.* 2001;21:893–901.
67. Reddy CE, Albanito L, De Marco P, Aiello D, Maggolini M, Napoli A, et al. Multisite phosphorylation of c-Jun at threonine 91/93/95 triggers the onset of c-Jun pro-apoptotic activity in cerebellar granule neurons. *Cell Death Dis.* 2013;4:e852.
68. Kozareva V, Martin C, Osorno T, Rudolph S, Guo C, Vanderburg C, et al. A transcriptomic atlas of mouse cerebellar cortex comprehensively defines cell types. *Nature.* 2021;598:214–19.
69. Kim MJ, Sang HP, Opella SJ, Marsilje TH, Michellys PY, Seidel HM, et al. NMR structural studies of interactions of a small, nonpeptidyl Tpo mimic with the thrombopoietin receptor extracellular juxtamembrane and transmembrane domains. *J Biol Chem.* 2007;282:14253–61.
70. Aggarwal BB. Signalling pathways of the TNF superfamily: a double-edged sword. *Nat Rev Immunol.* 2003;3:745–56.
71. Vilar M. Structural characterization of the p75 neurotrophin receptor. *Vitamins Hormones.* 2017;104:57–87.
72. Rudnick SA, Cadman EC, Capizzi RL, Skeel RT, Bertino JR, McIntosh S. High dose cytosine arabinoside (HDARAC) in refractory acute leukemia. *Cancer.* 1979;44:1189–93.
73. McLeod HL, Baker DK, Pui CH, Rodman JH. Somnolence, hypotension, and metabolic acidosis following high-dose teniposide treatment in children with leukemia. *Cancer Chemother Pharm.* 1991;29:150–4.
74. Kalinchuk AV, Porkka-Heiskanen T, McCarley RW. Basal forebrain and saporin cholinergic lesions: the devil dwells in delivery details. *Sleep.* 2006;29:1385–7.
75. Kalinchuk AV, McCarley RW, Stenberg D, Porkka-Heiskanen T, Basheer R. The role of cholinergic basal forebrain neurons in adenosine-mediated homeostatic control of sleep: Lessons from 192 IgG-saporin lesions. *Neuroscience.* 2008;157:238–53.
76. Kalinchuk AV, Porkka-Heiskanen T, McCarley RW, Basheer R. Cholinergic neurons of the basal forebrain mediate biochemical and electrophysiological mechanisms underlying sleep homeostasis. *Eur J Neurosci.* 2015;41:182–95.

## ACKNOWLEDGEMENTS

We thank Professor Carlos F Ibáñez for providing resources and insightful discussion. We also thank Dr Stella Nolte, Anne-Kerstine Glinthorg Jensen, Andreea-Cornelia Udrea, Sierra Lyn Wittrup Olsen, and Ket Yin Goh for excellent technical support. This research was supported by grants to LK from Karolinska Institute Research Foundation and Magnus Bergwall Foundation; PN from Lundbeck Foundation R310-2018-3713 and The Danish National Research Foundation grant DNR133; AN from The Danish National Research Foundation grant DNR133, Lundbeck Foundation R248-2017-431 and The Danish Council for Independent Research 7017-00261.

## AUTHOR CONTRIBUTIONS

VLR performed TM binding assay and Homo-FRET experiments. PB performed neurite degeneration and PLA experiments. MH did the docking experiment. DIP and LK performed the CESTA experiment. JCR and SLWO did the apoptotic dose–response experiment, and AA and DFS performed the initial experiments. PN provided advice and resources. LK conceived the study, planned, performed, and analysed most of the experiments. LK wrote the paper with input from all authors. All authors read and approved the final paper.

## COMPETING INTERESTS

The authors declare no competing interests.

## ETHICAL APPROVAL

All animal experiments were conducted in accordance with the National University of Singapore Institutional Animal Care, Use Committee and the Stockholm North Ethical Committee for Animal Research regulations and the Danish Animal Experiment Inspectorate Under the Ministry of Justice.

## ADDITIONAL INFORMATION

**Supplementary information** The online version contains supplementary material available at <https://doi.org/10.1038/s41419-023-05979-7>.

**Correspondence** and requests for materials should be addressed to Lilian Kisiswa.

**Reprints and permission information** is available at <http://www.nature.com/reprints>

**Publisher's note** Springer Nature remains neutral with regard to jurisdictional claims in published maps and institutional affiliations.



**Open Access** This article is licensed under a Creative Commons Attribution 4.0 International License, which permits use, sharing, adaptation, distribution and reproduction in any medium or format, as long as you give appropriate credit to the original author(s) and the source, provide a link to the Creative Commons license, and indicate if changes were made. The images or other third party material in this article are included in the article's Creative Commons license, unless indicated otherwise in a credit line to the material. If material is not included in the article's Creative Commons license and your intended use is not permitted by statutory regulation or exceeds the permitted use, you will need to obtain permission directly from the copyright holder. To view a copy of this license, visit <http://creativecommons.org/licenses/by/4.0/>.